

# Toward a Minimum Branching Fraction for Dark Matter Annihilation into Electromagnetic Final States

James B. Dent, Robert J. Scherrer, and Thomas J. Weiler

*Department of Physics and Astronomy,  
Vanderbilt University, Nashville, TN 37235, USA*

(Dated: February 2, 2022)

## Abstract

Observational limits on the high-energy neutrino background have been used to place general constraints on dark matter that annihilates only into standard model particles. Dark matter particles that annihilate into neutrinos will also inevitably branch into electromagnetic final states through higher-order tree and loop diagrams that give rise to charged leptons, and these charged particles can transfer their energy into photons via synchrotron radiation or inverse Compton scattering. In the context of effective field theory, we calculate the loop-induced branching ratio to charged leptons and show that it is generally quite large, typically  $\gtrsim 1\%$ , when the scale of the dark matter mass exceeds the electroweak scale,  $M_W$ . For a branching fraction  $\gtrsim 3\%$ , the synchrotron radiation bounds on dark matter annihilation are currently stronger than the corresponding neutrino bounds in the interesting mass range from 100 GeV to 1 TeV. For dark matter masses below  $M_W$ , our work provides a plausible framework for the construction of a model for “neutrinos only” dark matter annihilations.

While dark matter (DM) accounts for 25% of the total energy density in the universe (a classic review is [1]), direct detection remains elusive (see, e.g., Ref. [2] for a recent discussion). If the dark matter is a thermal relic, one would expect a non-negligible annihilation cross section, and one might hope to either detect the products of such annihilations occurring today, or to bound the properties of such particles by the non-observation of annihilation products.

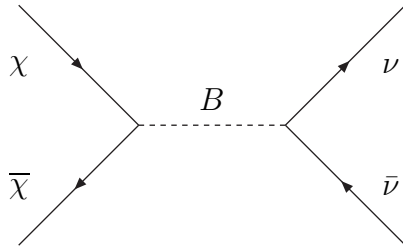
Recently, Beacom, Bell and Mack [3] made an interesting argument regarding such limits. They noted that if a dark matter particle ( $\chi$ ) couples only to Standard Model (SM) particles, then the most general limits can be derived by assuming annihilation into neutrinos, as these are the most difficult SM annihilation products to detect. Rather surprisingly, current observations place nontrivial bounds on such annihilations (see also Refs. [4, 5]). Mack et al. [6] compared these neutrino annihilation limits with corresponding limits on gamma-ray-producing annihilations. Their results indicate that, for an illustrative branching ratio to photons of  $10^{-4}$ , the neutrino bounds generally provide tighter constraints for large dark matter masses ( $M_\chi > 100$  MeV), while the photon bounds dominate at smaller masses. If the branching ratio into photons is taken to be larger, then the mass range over which the neutrino bounds dominate shrinks accordingly. Further, with the GLAST satellite [7] expected to launch in 2008, the photon limits will shortly be considerably tightened (or dark matter annihilation will be detected!).

Thus, it is very interesting to determine what constitutes a “reasonable” minimum branching ratio into electrically-charged particles, for these in turn generate photons. We will assume a “neutrinos only” final state at tree level, and then calculate the branching into charged leptons that results from a higher-order box diagram. Note that a calculation similar in spirit was undertaken by Kachelriess and Serpico [8], who examined the electromagnetic mode from electroweak bremsstrahlung of real  $W$  and  $Z$  particles. In quantitative detail [9], it is found that the branching fraction of this process is  $\frac{\alpha}{12\pi} \frac{M_\chi^2}{M_W^2} = 2.1 \times 10^{-4} \times \frac{M_\chi^2}{M_W^2}$ , for  $M_\chi \gtrsim M_W$  such that the electroweak bosons are produced on-shell; we have taken  $\alpha = 1/128$  for the numerical value, as is appropriate at the weak scale. The processes we discuss here are physically distinct from bremsstrahlung and offer a potentially more significant contribution to the electromagnetic branching ratio. In this work, we obtain a rate ratio from loop graphs growing as  $\left(\frac{\alpha M_\chi^2}{8\pi M_W^2}\right)^2$  times a logarithmic factor.

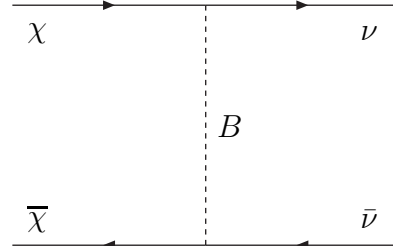
It is non-trivial to embed a tree-level “neutrinos only” final state model into a field theory.

The special status afforded the neutrino breaks the  $SU(2)$  invariance of the weak interaction. As a consequence, the embedded theory we construct must be viewed as incomplete, as an effective theory at best, valid up to some energy scale  $\Lambda$ . The effective theory will also be non-renormalizable, and therefore unstable against radiative corrections. This presents another indication that the neutrinos-only model exists only for a finely-tuned effective theory below a scale  $\Lambda$ , or for a UV-completed theory with a rich spectrum at  $\Lambda \sim M_B$ , where  $M_B$  is the mass scale of the interaction connecting the DM sector to neutrinos. The rich-spectrum possibility seems contrived and unlikely, but if true, it predicts much discovery not far beyond the energy reach of today's accelerators. We will assume that the neutrinos-only model is simple in a region of validity up to  $\Lambda^2 \gg M_B^2$ . We will present the consequences of such a model.

Assuming the dark matter to be fermions, we must at a minimum introduce a new scalar or vector boson particle/field  $B$ , with mass  $M_B$ , to mediate the dark matter annihilation to a neutrino-antineutrino pair. For the process  $\chi + \bar{\chi} \rightarrow \nu \bar{\nu}$  (here we are using the generic  $\nu$  to include all three neutrino flavors), one can imagine two types of vertices and diagrams: either an s-channel tree graph (I) with vertices mediated by  $\mathcal{L}_{\chi\chi B}$  and  $\mathcal{L}_{\nu\bar{\nu} B}$ , or a t-channel tree graph (II) with both vertices mediated by  $\mathcal{L}_{\chi B \nu}$ . A new quantum number is needed to elevate the  $\bar{\chi}\chi\bar{\nu}\nu$  operator to a privileged status, but we do not indulge in detailed model building here. Rather, we focus on the Standard Model (SM) loop-corrections to the diagrams (I) and (II).



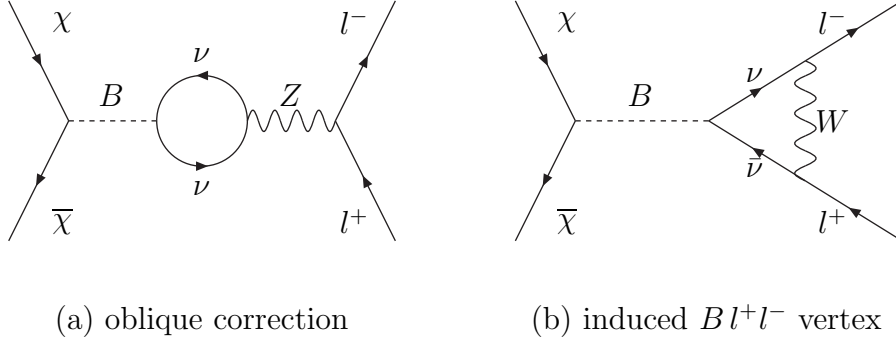
(I) s-channel B-exchange



(II) t-channel B-exchange

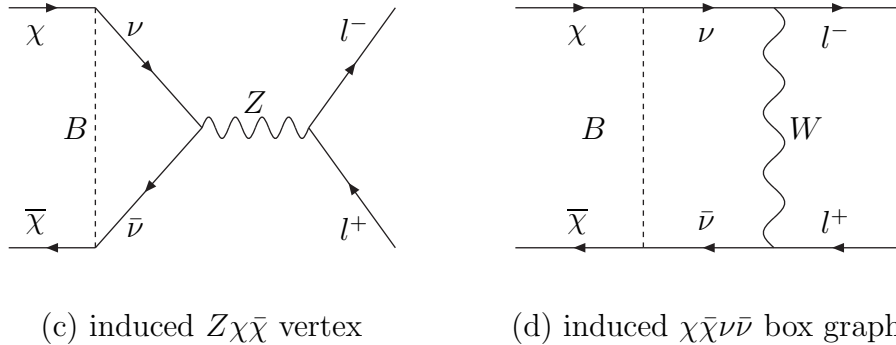
There are order  $(g^2)$  radiative corrections to the s-channel process which produce two-particle charged leptonic final states  $\sum_l l^+ l^-$ . Since we are comparing to the two-particle final states  $\sum_l \nu_l \bar{\nu}_l$ , the number of flavor generations will cancel from our results. For example, the ratio is unchanged whether the new interaction is assumed to produce all

three neutrino flavors, with concomitant induced production  $e^+e^-$ ,  $\mu^+\mu^-$ ,  $\tau^+\tau^-$ , or whether the new interaction is assumed to produce, say, just  $\nu_\tau\bar{\nu}_\tau$  with concomitant production of just  $\tau^+\tau^-$ . Corrections to the two-particle s-channel process are (a) s-channel Z-exchange, and (b) t-channel W-exchange. (These SM processes necessarily violate conservation of any charge carried by the  $B$  particle.)



The “oblique” correction in (a) induces  $B$ - $Z$  mixing. One may choose a counterterm to eliminate the mixing at one scale  $\mu$ . Although not natural, one can in principle choose the scale  $\mu$  to eliminate the mixing at the threshold  $\mu = 2M_\chi$ ; then, for non-relativistic DM, there is almost no production of  $l^+l^-$  from non-relativistic  $\chi$  annihilation. Similarly, the  $B l^+ l^-$  vertex correction in (b) can be canceled by a counterterm at one scale, e.g.  $\mu = 2M_\chi$ .

Radiative corrections to the t-channel process which produce an  $l^+l^-$  final state are an s-channel  $Z$ -exchange and a t-channel  $W$ -exchange.



In graph (c), the radiatively induced  $\chi \bar{\chi} Z$  vertex can be canceled by a counterterm at one value of  $\mu$ , say  $\mu = 2M_\chi$ . In contrast, the four-fermion vertex induced in graph (d) is of dimension six and has no counterterm. Thus, it must be rendered finite by direct calculation. The superficial degree of divergence in graph (a) is quadratic, (b) is quadratic

(in unitary gauge), (c) is logarithmic for scalar  $B$  and quadratic for vector  $B$  (in unitary gauge) and (d) is logarithmic for scalar  $B$  and quadratic for vector  $B$  (in unitary gauge). We now focus our attention on graph (d). We do so for two reasons. The first reason is that there is no counterterm for this graph to suppress the operator, and the second reason is that graph (d) is the least divergent of the graphs (along with (c)) and therefore represents a conservative window to our study of the stability of a “neutrinos only” model in the face of radiative corrections.

For our calculation, we make the simplest choice for the spin-parity of the  $B$ -meson, namely that it is a scalar particle. In fact, we show in Appendix I that the divergent contribution to the amplitude of the box graph factorizes into a divergent factor independent of the  $B$ -meson’s spin-parity, times a factor proportional to the tree-level amplitude. This latter factor depends on the  $B$ -meson’s spin-parity. However, this latter factor cancels in the ratio of box to tree amplitudes, which is what we investigate. Thus, our results are true for any spin-parity of the  $B$ -meson.

We render the box graph (d) finite by use of a Pauli-Villars (PV) regulator to compensate the  $B$  particle propagator. The Pauli-Villars cutoff  $\Lambda$  then becomes the maximum scale for a credible effective theory. We work in the unitary gauge, since this gauge, and only this gauge, includes only physical particles throughout the calculation. Thus, the only new parameter introduced is the PV regulator  $\Lambda$ , which now takes on the significance as the mass-scale above which additional new particles enter. Some details of our calculation in the unitary gauge are presented in Appendix (I). In Appendix (II) we calculate the same box graph in the general  $R_\xi$ -gauge, and compare the results to that from the unitary gauge calculation.

The amplitude for graph (d) depends on four dimensionful parameters,  $M_\chi$ ,  $M_B$ ,  $M_W$ , and  $\Lambda$ . Therefore, the ratio of rates (independent of the number of flavor generations)

$$\mathcal{R} = \frac{\langle v \sigma(\chi\bar{\chi} \rightarrow l^+l^-) \rangle}{\langle v \sigma(\chi\bar{\chi} \rightarrow \nu\bar{\nu}) \rangle} \quad (1)$$

depends on three independent ratios, which we may take to be  $M_\chi/M_W$ ,  $M_B/M_\chi$ , and  $\Lambda/M_B$ .  $M_W$  is known, of course. For the case of a thermal relic (only),  $M_\chi$  and  $M_B$  are constrained by the requirement that the  $\chi$  dark matter decouple from early universe thermal equilibrium such that  $\Omega_{DM}h^2 = 0.1$ , where  $h$  is the Hubble parameter in units of  $100 \text{ km sec}^{-1} \text{ Mpc}^{-1}$ . We will investigate this constraint below, in Eqs. (2-5).

The PV mass  $\Lambda$  is a priori a free parameter. Inherent in the PV regularization scheme

is vanishing of the electromagnetic amplitude at  $\Lambda = M_B$ . This results because the propagator for the fictitious unphysical  $\Lambda$  “particle” enters with the wrong sign, by construction. However, the spirit of the regularization is to produce a well-defined effective theory, valid up to the scale of the fictitious PV “particle”  $\Lambda \gg M_B$ . The higher the value of  $\Lambda$ , the more stable is the effective theory. We are therefore led to ask, at what value of  $\Lambda/M_B$  does the effective theory for the “neutrinos only” ansatz fail to support the idealized “neutrinos only” model? We answer this question with the graphs displayed in Figs. 1 and 2. If the theory fails at  $\Lambda$  not much larger than  $2M_\chi$ , then the field theory is very incomplete as written; more fields are needed already near the dark matter scale  $M_\chi$ . With more fields come more counterterms. Consequently, more fine tuning of these counterterms is needed to maintain the “neutrinos only” model. It seems more likely that nature eschews this additional tedium, and the electromagnetic branching ratio increases at scales  $\gtrsim \Lambda$ .

In Figs. 1 and 2 we show the ratio  $\mathcal{R}$  of annihilation rates into  $l^+l^-$  (through the box diagram) versus into  $\nu\bar{\nu}$ , as a function of the cutoff scale (in units of  $M_B$ ), with  $M_B$  taken to be 10 and 20 times the  $W$  mass, respectively, and for  $M_\chi$  taken to be 2, 5, and 10 times  $M_W$ . In calculating the box graph, we have neglected complicating non-leading contributions, as they are unnecessary for the thesis of this paper. From the figures, one sees that already at  $\Lambda \sim 3$  times  $M_B$ , the relative rate into the  $l^+l^-$  mode is of order 1%. In fact, we may invoke the simple asymptotic formula in Eq. (19) to infer that the rate ratio  $\mathcal{R}$  grows as  $\ln^2(\Lambda/M_B)$ , and that a somewhat minimal mass ordering  $\Lambda \sim 10 M_B \sim 10^2 M_W$  will necessarily yield  $\mathcal{R} \sim$  few percent.

Our results for the ratio  $\mathcal{R}$  of rates versus the  $\chi$  mass are shown in Figs. 3 and 4. We note that  $\mathcal{R}$  is an increasing function of  $M_\chi$ , of  $\Lambda/M_B$ , and of  $M_B/M_W$ , as shown explicitly in Eq. (17). We note that the monotonic increase of the rate ratio with  $\Lambda$  is an inevitable consequence of PV regularization, and the increase with  $M_\chi$  and  $M_B$  derives from the propagator suppression of the tree-level rate,  $\sim (t - M_B^2)^{-2} \approx (-M_\chi^2 - M_B^2)^{-2}$ . Fortunately, it is precisely the most physically-reasonable values for these parameters that yield the largest electromagnetic branching ratio. For a reasonable renormalization scheme, we would want  $\Lambda \gg M_B$ . Further,  $M_B/M_W$  must be large enough to avoid heretofore undetected new physics [10].

It is also interesting to determine the constraints which apply to our parameters if  $\chi$  is a thermal relic. In this case,  $M_B$  and  $M_\chi$  are constrained by the requirement that the  $\chi$

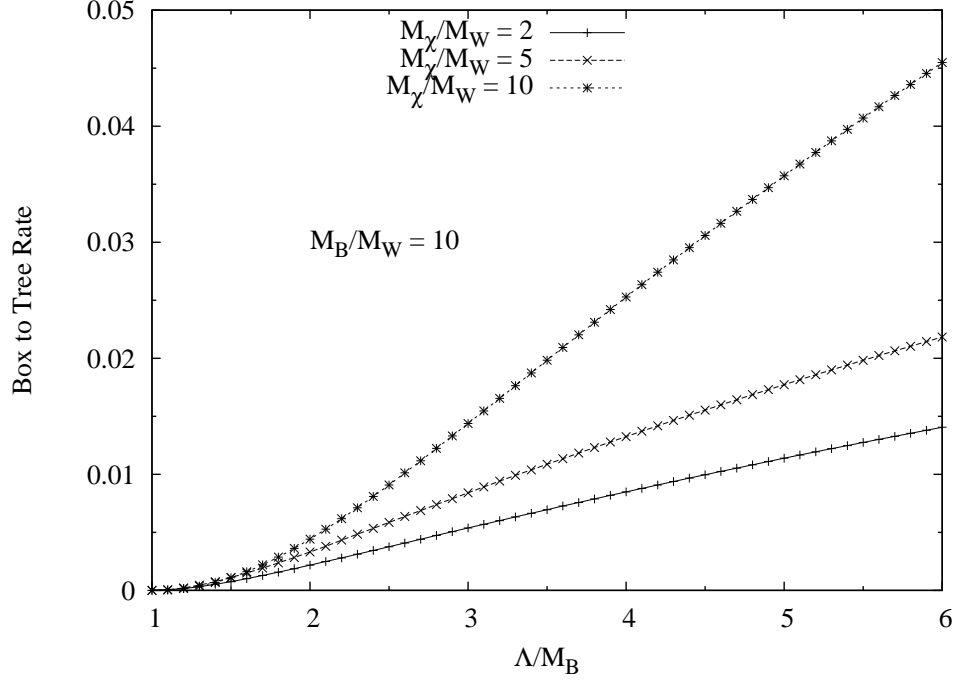


FIG. 1: The ratio of the rate for  $\chi\chi \rightarrow l^+l^-$  from the box diagram to the rate for  $\chi\chi \rightarrow \bar{\nu}\nu$  at tree level, as a function of  $\Lambda/M_B$ , where  $\Lambda$  is the cutoff scale of the effective theory and  $M_B$  is the mass of the boson that mediates the  $\chi$  annihilation into neutrinos. Here,  $M_B/M_W = 10$ , and  $M_\chi/M_W$  has the values 2, 5, and 10.

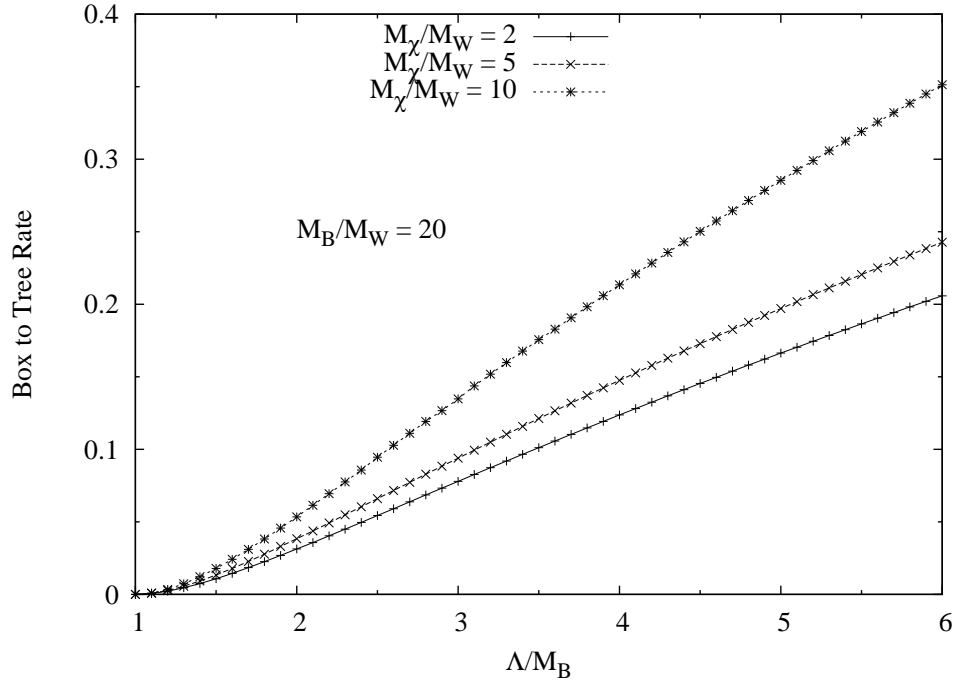


FIG. 2: As Fig. 1, but with  $M_B/M_W = 20$ .

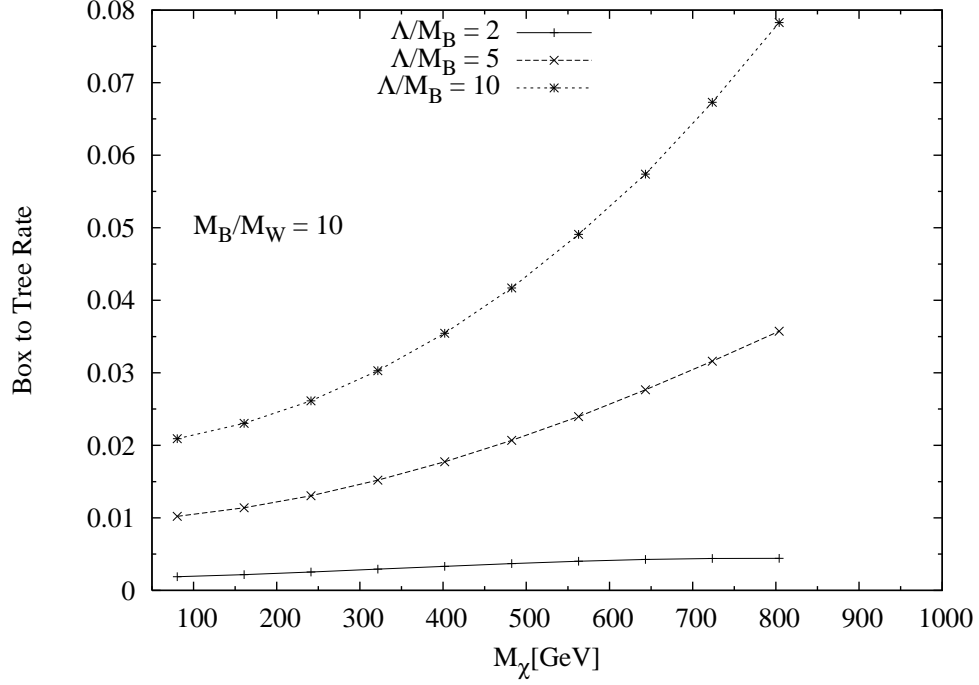


FIG. 3: The ratio of the rate for  $\chi\chi \rightarrow l^+l^-$  from the box diagram to the rate for  $\chi\chi \rightarrow \bar{\nu}\nu$  at tree level, as a function of the  $\chi$  mass, for  $M_B/M_W = 10$  and  $\Lambda/M_B = 2, 5$ , and  $10$ .  $M_B$  is the mass of the boson that mediates the  $\chi$  annihilation into neutrinos, and  $\Lambda$  is the cut-off scale of the effective theory.

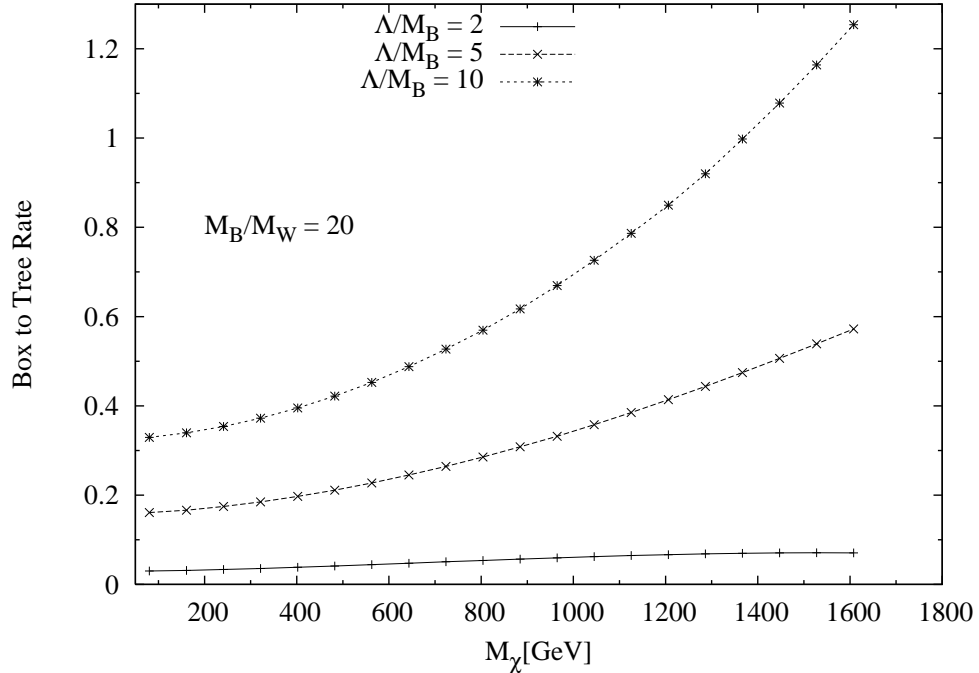


FIG. 4: As Fig. 3, but with  $M_B/M_W = 20$ .



abundance account for the currently observed dark matter: the value  $\Omega_\chi h^2 = 0.1$  requires an annihilation rate of approximately  $\langle v\sigma \rangle \sim 3 \times 10^{-26} \text{ cm}^3 \text{ sec}^{-1}$  for thermally-produced dark matter [1, 11]. In the model presented here, in the non-relativistic limit  $s \sim (2 M_\chi)^2$  and large  $M_B^2 \gg s$  limit, we have

$$\langle v\sigma \rangle \times Br(\chi\bar{\chi} \rightarrow \nu\bar{\nu}) = \left(\frac{g_B^4}{4\pi}\right) \left(\frac{M_\chi^2}{M_B^4}\right) \quad (2)$$

for the pure  $L = 0$  partial wave  $s$ -channel exchange of the  $B$ , and  $\sim \frac{1}{2}$  times this for  $t$ -channel  $B$  exchange (where an  $L = 1$  contribution to the rate is suppressed by the square of the  $\chi$  velocity);  $Br(\chi\bar{\chi} \rightarrow \nu\bar{\nu})$  is the annihilation branching ratio to  $\nu\bar{\nu}$ . Substituting the desired rate for  $\langle v\sigma \rangle$  into this equation, and taking  $Br(\chi\bar{\chi} \rightarrow \nu\bar{\nu}) = 1$ , we obtain the result

$$\left(\frac{4\pi}{g_B^2}\right) \left(\frac{M_B}{M_\chi}\right)^2 M_\chi = 70 \text{ TeV}, \quad (3)$$

or

$$\frac{M_B}{M_\chi} = 26 \sqrt{\left(\frac{g_B^2}{4\pi}\right) \left(\frac{100 \text{ GeV}}{M_\chi}\right)}. \quad (4)$$

If we consider only  $M_\chi > 100 \text{ GeV}$ , and restrict the coupling to the perturbative regime  $g_B^2 \leq 4\pi$ , then we obtain the bound [29]

$$1 < \frac{M_B}{M_\chi} < 26, \quad (5)$$

where the lower bound comes from the additional requirement that  $M_\chi < M_B$  so that the  $\chi$  dark matter is not de-stabilized by the simple decay chain  $\chi \rightarrow B + \nu$  [30]. Thus, the mass of the boson  $B$  cannot be wildly larger than that of the dark matter particle. (When the box-diagram annihilation rate into  $l^+l^-$  becomes significant, the value of  $Br(\chi\bar{\chi} \rightarrow \nu\bar{\nu}) < 1$  must be included in the algebra.) Of course, if the dark matter is not a thermal relic, then these constraints no longer apply. None of the other results in this paper rely on the assumption that  $\chi$  is a thermal relic, and of course, the constraints on  $\langle v\sigma \rangle$  that we examine later in the paper are irrelevant if  $\langle v\sigma \rangle$  is fixed to give the thermal relic abundance.

We have presented figures only for the case where  $M_\chi > M_W$ . However, the calculation in Appendix (I) is valid for the case  $M_\chi < M_W$  as well. In this case, we find that the branching into  $l^+l^-$  is infinitesimal. However, as we have not included the induced  $Z\chi\bar{\chi}$  vertex shown in Fig. (c) in the calculation of the annihilation rate into  $\nu\bar{\nu}$ , we cannot offer a reliable estimate of the rate if  $M_\chi < M_W$ . A calculation of the contribution of the vertex

diagram to the total annihilation rate is irrelevant to conclusions of the present paper, but would be needed to extend the framework presented here to a more complete “neutrinos only” annihilation model for  $M_\chi < M_W$ .

Returning to the case  $M_\chi > M_W$ , our results indicate that a model for dark matter annihilation that produces only neutrinos at tree level, when sensibly embedded into a field theory, will produce a significant ( $> 1\%$ ) branching into  $l^+l^-$ . It is reasonable to ask whether such a branching ratio is large enough to provide limits competitive with the neutrino limits discussed in Refs. [3, 4, 6]. The neutrino annihilation limits in Ref. [3] are for cosmic dark matter annihilations, while the (tighter) limits from Ref. [4] are for annihilations in the halo of the galaxy; it is the latter which we will consider here. (Palomares-Ruiz and Pascoli [5] consider neutrino constraints for dark matter masses below 100 MeV, outside of the mass range for which our results are interesting). Ref. [6] also provides general limits on annihilation into high-energy photons. These limits are not directly applicable to our calculation, since we consider branching into charged leptons rather than photons. High-energy leptons will convert their energy into photons primarily through inverse Compton scattering off of background photons, or, if a magnetic field is present, through synchrotron radiation. For our purposes, it is sufficient to consider only the latter effect, within the Galaxy, where the magnetic field is reasonably well known. For discussions of the former effect, see, e.g., Refs. [12, 13, 14, 15, 16]. (See also Ref. [17] for one of the earliest discussions of these phenomena).

Synchrotron radiation from the products of dark matter annihilation has been investigated in some detail [12, 13, 14, 18, 19, 20, 21, 22, 23]. More recently, it has been suggested that the microwave “haze” near the center of the Galaxy, observed by WMAP, could be synchrotron radiation from such annihilations [24, 25, 26]. Finally, Hooper [27] has used the WMAP observations to bound annihilation-produced synchrotron radiation. This latter result can be combined with our predicted branching ratio into charged leptons and compared with the corresponding neutrino bounds.

Our results allow branching into  $e^+e^-$ ,  $\mu^+\mu^-$ , or  $\tau^+\tau^-$ , depending on the neutrinos that couple in  $\mathcal{L}_{\chi B\nu}$ . Synchrotron radiation is produced directly by  $e^+e^-$ , and indirectly through the decay-produced electrons from  $\mu^+\mu^-$  and  $\tau^+\tau^-$ . In the latter two cases, some of the decay energy goes into neutrinos and does not contribute to the synchrotron radiation. Thus, the  $e^+e^-$  annihilation channel yields the strongest synchrotron signal, followed by  $\mu^+\mu^-$  and

then  $\tau^+\tau^-$  [25]. Since we make no prediction for the specific type of neutrinos produced by the dark matter annihilations, we can derive the most conservative limits by considering annihilation into  $\tau^+\tau^-$  only.

Hooper [27] gives limits on the cross-section for dark matter annihilation into  $\tau^+\tau^-$  using the requirement that the resulting synchrotron radiation not exceed the WMAP microwave observations near the center of the Galaxy. He presents two sets of limits, the first corresponding to an assumed Navarro-Frenk-White (NFW) profile [28], and the second to an assumed uniform distribution of the dark matter inside of the solar circle. Similarly, Yuksel et al. [4] give three different sets of limits based on the angular scale over which the neutrino emission is measured, and they provide appropriate modification factors for each limit assuming any of three density profiles. While there is no exact correspondence between any of the limits provided in Ref. [27] and those given in Ref. [4], the closest correspondence is between the NFW synchrotron limit in Ref. [27] and the “Halo Angular” limit in Ref. [4], for the parameters appropriate to the NFW profile. Comparing these two sets of limits for annihilation purely into  $\tau^+\tau^-$ , with  $M_\chi = 100$  GeV, we find that the upper bound on  $\langle v\sigma \rangle$  from  $\bar{\nu}\nu$  production is roughly 1000 times the corresponding limit from  $\tau$ -produced synchrotron radiation. This ratio decreases to about 30 at  $M_\chi = 1$  TeV. Thus, the synchrotron bounds from the production of charged leptons are tighter than the neutrino bounds at  $M_\chi \sim 100$  GeV if the branching ratio to charged leptons is  $\gtrsim 0.1\%$ . For  $M_\chi \sim 1$  TeV, this branching ratio must be  $\gtrsim 3\%$  in order for the synchrotron bounds to be tighter than the neutrino bounds. This is the mass range ( $100 \text{ GeV} \lesssim M_\chi \lesssim 1 \text{ TeV}$ ) of greatest interest from the point of view of WIMP dark matter. (Strictly speaking, the neutrinos from  $\tau$  decay should be included in the total neutrino signal when comparing to the neutrino limits in Ref. [4], but this is a small effect as long as the branching ratio into charged leptons is  $\ll 1$ ).

Our results do not undercut the neutrino limits proposed in Refs. [3, 4, 5]; these certainly remain valid limits on the annihilation rate for dark matter. Further, it is clear that both the synchrotron limits derived in Ref. [27] and the neutrino limits in Ref. [4] depend on the assumed model for the distribution of dark matter in the Galaxy. However, our purpose in this paper is not to determine the exact ratio between these two sets of limits (which may change with improved observations or more detailed calculations in any case) but simply to point out that the neutrino and charged lepton/photon sensitivities are likely to be competitive with each other over the WIMP mass range of greatest interest. For dark

matter masses below the  $W$  mass, we can offer no useful new limits. Our calculations in this case allow annihilation into neutrinos only, with only an infinitesimal branching to other particles.

Although our results might seem to be limited to the specific model we have examined, they are rather general. Whenever neutrino-antineutrino pairs are produced in the final state, they can always be converted into  $l^+l^-$  pairs through  $Z$  or  $W$  exchange as in diagrams (a) to (d) above. This is an inevitable consequence of the Standard Model; no new physics is required. The only assumption concerns the creation of a specific interaction that couples dark matter to  $\nu\bar{\nu}$  pairs at tree level. Once such a model is in place, however, the induced coupling to  $l^+l^-$  is inevitable and readily calculable.

### Acknowledgments

J.B.D., R.J.S., and T.J.W. were supported in part by the Department of Energy (DE-FG05-85ER40226). We thank J. Beacom, D. Hooper, and G. Mack for helpful discussions.

## I. APPENDIX: CALCULATION OF BOX DIAGRAM (IN UNITARY GAUGE) AND ELECTROMAGNETIC RATE

Here we present the amplitude for the box diagram of Figure (d), and a calculation of the divergent part of this amplitude. Then we construct the ratio of rates,

$$\mathcal{R} = \left[ \frac{\langle v \sigma(\chi\bar{\chi} \rightarrow l^+l^-) \rangle}{\langle v \sigma(\chi\bar{\chi} \rightarrow \nu\bar{\nu}) \rangle} \right]_{DivPart}. \quad (6)$$

The subscripted qualifier “DivPart” is a reminder that only the leading (divergent) contribution to the electromagnetic rate will be included here.

In unitary gauge, the  $W$ -propagator is

$$\frac{-i(g_{\mu\nu} - k_\mu k_\nu / M_W^2)}{k^2 - M_W^2 + iM_W\Gamma_W}, \quad (7)$$

and the matrix element for the amplitude of the box (d) is given by

$$\begin{aligned} i\mathcal{M}_{\text{box}} = & \int \frac{d^4k}{(2\pi)^4} \left( \frac{i}{(k-p+q)^2 - M_B^2 + iM_B\Gamma_B} \right) \left( \frac{-i(g_{\mu\nu} - k_\mu k_\nu / M_W^2)}{k^2 - M_W^2 + iM_W\Gamma_W} \right) \\ & \times \left( \frac{i}{(k+q)^2 - M_\nu^2 + i\epsilon} \right) \left( \frac{i}{(\bar{q}-k)^2 - M_\nu^2 + i\epsilon} \right) \end{aligned} \quad (8)$$

$$\times [\bar{u}(q)\Gamma_W^\mu(\not{k} + \not{q} + M_\nu)\Gamma_B u(p)] [\bar{v}(\bar{p})\Gamma_B(\not{q} - \not{k} + M_\nu)\Gamma_W^\nu v(\bar{q})],$$

where the momenta assignments to the particles are  $\chi(p)$ ,  $\bar{\chi}(\bar{p})$ ,  $l^-(q)$ ,  $l^+(\bar{q})$ ,  $W(k)$ , which in turn determine the further assignments  $B(k - p + q)$ ,  $\nu(k + q)$ , and  $\bar{\nu}(\bar{q} - k)$ . Here  $\Gamma_W^\mu = (\frac{g}{\sqrt{2}})\gamma^\mu \frac{(1-\gamma_5)}{2}$  is the usual charged-current electroweak vertex with the  $SU(2)$  coupling constant  $g = e/\sin\theta_w$ ,  $p$  is the four-momentum of the dark matter,  $q$  is the four-momentum of the electron, and the internal loop four-momentum of the virtual  $W$ -boson is given by  $k$ . In addition,  $\Gamma_B$  in the numerator is the coupling times Lorentz structure assigned to a  $B\chi\nu$  vertex, not to be identified with the  $B$  width in the denominator. The value of the coupling we do not require, as the coupling cancels out when divided by the amplitude of the tree diagram; accordingly, we let simplicity be our guide and choose a scalar Lorentz structure for the  $B$  field. We will neglect the neutrino and charged lepton masses, and define  $M_\chi$  to be the dark matter mass.

We introduce four Feynman parameters  $\xi_i$  (one per internal line) and find for the denominator  $D$ :

$$\begin{aligned} \frac{1}{D} = & (4-1)! \int_0^1 d\xi_1 \int_0^1 d\xi_2 \int_0^1 d\xi_3 \int_0^1 d\xi_4 \delta(1 - [\xi_1 + \xi_2 + \xi_3 + \xi_4]) \\ & \times [\xi_1((k - p + q)^2 - M_B^2) + \xi_2(k^2 - M_W^2) + \xi_3(k + q)^2 + \xi_4(k - \bar{q})^2]^{-4} \end{aligned} \quad (9)$$

Here we have dropped the  $B$  and  $W$  widths from the denominator, as they play no important role in the present calculation. Upon rotating  $k$  to Euclidean space, we find that the divergent part of the amplitude, coming from the longitudinal mode of the  $W$  propagator, is

$$\mathcal{M}_{\text{box}} = \frac{-g^2}{8M_W^2} \int \frac{d^4 k_E}{(2\pi)^4} \int d\xi \frac{k_E^4}{(k_E^2 + \Delta_B^2)^4} \times [\bar{u}(q)(1 + \gamma_5)\Gamma_B u(p)] [\bar{v}(\bar{p})\Gamma_B(1 - \gamma_5)v(\bar{q})]. \quad (10)$$

Here we have defined the functional

$$\begin{aligned} \int d\xi & \equiv 3! \int_0^1 d\xi_1 \int_0^1 d\xi_2 \int_0^1 d\xi_3 \int_0^1 d\xi_4 \delta(1 - [\xi_1 + \xi_2 + \xi_3 + \xi_4]) \\ & = 6 \left[ \int_0^1 d\xi_1 \int_0^{1-\xi_1} d\xi_2 \int_0^{1-\xi_1-\xi_2} d\xi_3 \right]_{\xi_4=1-\xi_1-\xi_2-\xi_3} \end{aligned} \quad (11)$$

and the parametrized mass-squared

$$\Delta_B^2 \equiv \xi_1 M_B^2 + \xi_2 M_W^2 - (\xi_1 - \xi_1^2 - 2\xi_1\xi_2 + 4\xi_3\xi_4) M_\chi^2. \quad (12)$$

In (12) we have set the invariant  $t \equiv (q - p)^2$  equal to the value appropriate for a non-relativistic  $\chi\bar{\chi}$  annihilation, namely,  $t \approx -M_\chi^2$ .

Performing the integral over  $k_E$  will result in a logarithmic divergence, and therefore we introduce a Pauli-Villars regulator for the  $B$  propagator

$$\frac{i}{(k - p + q)^2 - M_B^2} \rightarrow \frac{i}{(k - p + q)^2 - M_B^2} - \frac{i}{(k - p + q)^2 - \Lambda^2} \quad (13)$$

As is well-known, the Pauli-Villars regularization preserves local and global symmetries of the interaction. We then perform the integral over  $k_E$ , and find that the divergent amplitude after regularization becomes

$$\mathcal{M}_{\text{box}} = \frac{-g^2}{2^7 \pi^2 M_W^2} [\bar{u}(q)(1 + \gamma_5)\Gamma_B u(p)] [\bar{v}(\bar{p})\Gamma_B(1 - \gamma_5)v(\bar{q})] \int d\xi \ln \left| \frac{\Delta_\Lambda^2}{\Delta_B^2} \right|, \quad (14)$$

where

$$\Delta_\Lambda^2 = \Delta_B^2(M_B^2 \rightarrow \Lambda^2) = \xi_1 \Lambda^2 + \xi_2 M_W^2 - (\xi_1 - \xi_1^2 - 2\xi_1\xi_2 + 4\xi_3\xi_4) M_\chi^2. \quad (15)$$

Due to the assumed scalar nature of the  $B$  particle, the  $\gamma_5$ 's in Eq. (14) may be omitted.

The tree-level amplitude for  $\chi\bar{\chi} \rightarrow \nu\bar{\nu}$  is

$$i\mathcal{M}_{\text{tree}} = [\bar{u}(q)\Gamma_B u(p)] \left( \frac{i}{t - M_B^2} \right) [\bar{v}(\bar{p})\Gamma_B v(\bar{q})]. \quad (16)$$

Dividing the box amplitude by the tree-level amplitude (with  $t \approx -M_\chi^2$ , again) and squaring, we arrive at the result

$$\mathcal{R} = \left( \frac{M_B^2 + M_\chi^2}{128 \cdot 8\pi \cdot M_W^2} \right)^2 \left[ \int d\xi \ln \left| \frac{\Delta_\Lambda^2}{\Delta_B^2} \right| \right]^2. \quad (17)$$

For the running  $SU(2)$  coupling we use the value applicable at the weak scale:

$$g^2 = \frac{e^2}{\sin^2 \theta_w} \approx 4 e^2 = 16\pi \alpha \approx \frac{16\pi}{128}. \quad (18)$$

Notice that the spin-parity assignment of the  $B$ -meson appears only via the Dirac structure  $\Gamma_B$ , which cancels out of the ratio  $\mathcal{R}$ . Thus, our results to follow are independent of the  $B$ -meson's spin and parity.

There are some interesting, exactly calculable limiting cases. For  $M_B^2 \gg M_\chi^2$ ,  $M_W^2$ , one has  $\Delta_\Lambda^2/\Delta_B^2 \approx \Lambda^2/M_B^2$ , independent of  $\int d\xi$ , and so Eq. (17) becomes to lowest non-vanishing order, simply

$$\mathcal{R} \longrightarrow 0.97 \times 10^{-7} \left( \frac{M_B}{M_W} \right)^4 \left[ \ln \left( \frac{\Lambda^2}{M_B^2} \right) \right]^2, \quad \text{for } M_B^2 \gg M_\chi^2, M_W^2. \quad (19)$$

We note that Eq. (5) allows this mass ordering, but does not require it.

Another interesting calculable limit is  $M_\chi^2 \ll M_B^2, \Lambda^2, M_W^2$ . Neglecting  $M_\chi^2$  in  $\Delta_B^2$  and  $\Delta_\Lambda^2$ , one finds that to lowest non-vanishing order,

$$\mathcal{R} \longrightarrow \left( \frac{M_B^2}{128 \cdot 8\pi \cdot M_W^2} \right)^2 \left[ \ln \left( \frac{\Lambda^2}{M_B^2} \right) + \frac{\ln \left( \frac{M_W^2}{\Lambda^2} \right)}{\left( 1 - \frac{\Lambda^2}{M_W^2} \right)} - \frac{\ln \left( \frac{M_W^2}{M_B^2} \right)}{\left( 1 - \frac{M_B^2}{M_W^2} \right)} \right]^2, \text{ for } M_\chi^2 \ll M_B^2, \Lambda^2, M_W^2. \quad (20)$$

If in addition to  $M_\chi^2 \ll M_B^2, \Lambda^2, M_W^2$ , one includes  $M_B^2, \Lambda^2 \ll M_W^2$ , i.e., a low-mass model with a low-mass cutoff, then there results

$$\mathcal{R} \rightarrow 0.97 \times 10^{-7} \left( \frac{M_B}{M_W} \right)^4 \left[ \left( \frac{\Lambda^2}{M_W^2} \right) \ln \left( \frac{M_W^2}{\Lambda^2} \right) - \left( \frac{M_B^2}{M_W^2} \right) \ln \left( \frac{M_W^2}{M_B^2} \right) \right]^2, \text{ for } M_\chi^2 \ll M_B^2, \Lambda^2 \ll M_W^2. \quad (21)$$

Another limit, for a low-mass model with a high-mass cutoff, is

$$\mathcal{R} \rightarrow 0.97 \times 10^{-7} \left( \frac{M_\chi^2 + M_B^2}{M_W^2} \right)^2 \left[ \frac{\ln \left( \frac{\Lambda^2}{M_W^2} \right)}{\left( 1 - \frac{M_W^2}{\Lambda^2} \right)} \right]^2, \quad \text{valid for } M_\chi^2, M_B^2 \ll \Lambda^2, M_W^2. \quad (22)$$

The bracketed quantity in (22) is a monotonically increasing function of  $\Lambda/M_W$ , equal to zero at  $\Lambda = 0$  (as it must at  $\Lambda = M_B$ ), to 1 at  $\Lambda = M_W$ , and growing as  $\ln(\Lambda^2/M_W^2)$  at  $\Lambda^2 \gg M_W^2$ . It is clear that with the ordering  $M_B^2 \ll M_W^2$ , i.e., when the tree graph has a light-mass ( $M_B$ ) propagator while the box graph has a heavy-mass ( $M_W$ ) propagator, then the resulting electromagnetic branching fraction is negligible for any value of the effective field theory cutoff  $\Lambda$ , even up to the Planck mass.

## II. APPENDIX: CALCULATION OF BOX DIAGRAM IN $R_\xi$ GAUGE

Given that the unitary gauge admits only the three physical  $W$  spin states into the  $W$  propagator, this gauge choice is guaranteed to produce diagrams whose cuttings respect the Cutkowsky rules; other gauges will not. Nevertheless, the “renormalizable  $R_\xi$  gauges”, rather than the unitary gauge, are often invoked because their resulting propagators offer a more benign high-energy behavior. Of course, when a gauge invariant set of graphs is summed to calculate an  $S$ -matrix element, all gauges must give the same gauge-invariant ( $\xi$ -independent) answer. However, the box graph of interest here is not itself gauge invariant, the reason being that the dark sector breaks electroweak gauge invariance by treating the

neutrino differently from its  $SU(2)$  charged lepton partner. Consequently, we expect the box graph to yield a gauge-dependent answer. We have dealt with this situation in the main text by arguing that the unitary gauge is singled out since it, and it alone, includes only physical  $W$  states in its Feynman rules. Nevertheless, it is interesting and instructive to calculate the box graph in a general  $R_\xi$  gauge. We do that here.

The unitary gauge  $W$ -propagator, given in Eq. (7), is the  $\xi \rightarrow \infty$  limit of the general  $R_\xi$ -gauge  $W$ -propagator (we neglect the finite  $W$ -width)

$$D_{\mu\nu}^W(\xi) = \left( \frac{-i}{k^2 - M_W^2} \right) \left( g_{\mu\nu} - \frac{k_\mu k_\nu (1 - \xi)}{k^2 - \xi M_W^2} \right), \quad (23)$$

and the accompanying unphysical Goldstone boson propagator is

$$D_{GB}(\xi) = \frac{+i}{k^2 - \xi M_W^2}. \quad (24)$$

In contrast to the calculation in the unitary gauge where the leading high-energy behavior was given by a logarithmic divergence, here, for any finite  $\xi$ , the leading high energy contribution to the box graph is finite and therefore calculable. However, the result will be gauge ( $\xi$ ) dependent. To facilitate the calculation, we note that (i) the Goldstone boson contribution to the amplitude does not contribute to the leading high-energy behavior, and so will be neglected, and (ii) the  $R_\xi$  gauge  $W$ -propagator (Eq. 23) can be rewritten as a sum of the  $\xi$ -independent unitary gauge propagator and a  $\xi$ -dependent correction:

$$D_{\mu\nu}^W(\xi) = \frac{-i (g_{\mu\nu} - k_\mu k_\nu / M_W^2)}{k^2 - M_W^2} + \frac{+i (-k_\mu k_\nu / M_W^2)}{k^2 - \xi M_W^2}. \quad (25)$$

As far as the high-energy behavior of the amplitude is concerned, the contribution from the unitary gauge  $W$ -propagator again yields  $\Delta_B^2$  in Eq. (12), which we rename  $\Delta_W^2$  to emphasize the role of the physical  $W$ -propagator in this contribution. The additional contribution from the “wrong sign” propagator with a pole at the Goldstone boson mass-squared  $\xi M_W^2$  yields

$$\Delta_{GB}^2 \equiv \xi_1 M_B^2 + \xi_2 (\xi M_W^2) - (\xi_1 - \xi_1^2 - 2\xi_1 \xi_2 + 4\xi_3 \xi_4) M_\chi^2. \quad (26)$$

We then have

$$\mathcal{R} = \left( \frac{M_B^2 + M_\chi^2}{128 \cdot 8\pi \cdot M_W^2} \right)^2 \left[ \int d\xi \ln \left| \frac{\Delta_{GB}^2}{\Delta_W^2} \right| \right]^2. \quad (27)$$

The bracketed expression here,  $\int d\xi \ln \left| \frac{\Delta_{GB}^2}{\Delta_W^2} \right|$ , is bounded by  $\ln \left| \frac{\xi m_W^2}{M_W^2} \right| = \ln |\xi|$ . We see that the fictitious Goldstone boson mass-squared  $\xi M_W^2$  has come to play the role in the  $R_\xi$ -gauge



calculation that the fictitious PV mass-squared  $\Lambda^2$  played in the unitary gauge calculation. As a consistency check, we see that both  $\xi \rightarrow \infty$  and  $\Lambda^2 \rightarrow \infty$  return the infinite unitary gauge contribution without PV regularization.

This result explicitly demonstrates the merit of using the unitary gauge and a Pauli-Villars regularization scheme for the divergent graph. The particle degrees of freedom in the unitary gauge are all physical, and the PV cutoff  $\Lambda$  has physical meaning.  $\Lambda$  is the scale up to which the model is applicable, and beyond which the ultraviolet completion of the theory cannot be ignored. In contrast, the cutoff provided by the Goldstone mass in the renormalizable gauges has no physical interpretation.

- 
- [1] G. Jungman, M. Kamionkowski, and K. Griest, Phys. Rep. **267**, 195 (1996).
  - [2] G. Bertone, D. Hooper, and J. Silk, Phys. Rep. **405**, 279 (2005).
  - [3] J.F. Beacom, N.F. Bell, and G.D. Mack, Phys. Rev. Lett. **99**, 231301 (2007).
  - [4] H. Yuksel, S. Horiuchi, J.F. Beacom, and S. Ando, Phys. Rev. D **76**, 123506 (2007).
  - [5] S. Palomares-Ruiz and S. Pascoli, Phys. Rev. D **77**, 025025 (2008).
  - [6] G.D. Mack, T.D. Jacques, J.F. Beacom, N.F. Bell, and H. Yuksel, arXiv:0803.0157.
  - [7] GLAST Collaboration, <http://www-glast.stanford.edu>
  - [8] M. Kachelriess and P. D. Serpico, Phys. Rev. D **76**, 063516 (2007).
  - [9] N.F. Bell, J.B. Dent, T.D. Jacques, and T.J. Weiler, arXiv:0805.3423.
  - [10] There is also a constraint on “secret” self-interactions of neutrinos, coming from the observed invisible width of the  $Z$  boson: M. S. Bilenky and A. Santamaria, arXiv:hep-ph/9908272. However, this constraint turns out to be that the  $\nu\bar{\nu}\nu\bar{\nu}$  operator be as weak or weaker than the SM Fermi coupling  $G_F$ . In contrast, the dark matter operator  $\chi\bar{\chi}\nu\bar{\nu}$  is already of weak strength, so the loop-induced  $\nu\bar{\nu}\nu\bar{\nu}$  operator obtained by “squaring”  $\chi\bar{\chi}\nu\bar{\nu}$  and integrating out the  $\chi$  and  $\bar{\chi}$  would be much smaller.
  - [11] R.J. Scherrer and M.S. Turner, Phys. Rev. D **33**, 1585 (1986).
  - [12] E.A. Baltz and L. Wai, Phys. Rev. D **70**, 023512 (2004).
  - [13] S. Colafrancesco, S. Profumo, and P. Ullio, Astron. Astrophys. **455**, 21 (2006).
  - [14] S. Colafrancesco, S. Profumo, and P. Ullio, Phys. Rev. D **75**, 023513 (2007).
  - [15] S. Profumo, Phys. Rev. D **77**, 103510 (2008).

- [16] T.E. Jeltema and S. Profumo, arXiv:0805.1054.
- [17] Ya. B. Zeldovich, A.A. Klypin, M. Yu. Khlopov, and V.M. Chechetkin, Sov. J. Nucl. Phys. **31**, 664 (1980).
- [18] V. Berezhinsky, A.V. Gurevich, and K.P. Zybin, Phys. Lett. B **294**, 221 (1992).
- [19] V. Berezhinsky, A. Bottino, and G. Mignola, Phys. Lett. B **325**, 136 (1994).
- [20] P. Gondolo, Phys. Lett. B **494**, 181 (2000).
- [21] G. Bertone, G. Sigl, and J. Silk, Mon. Not. Roy. Astr. Soc. **326**, 799 (2001).
- [22] P. Blasi, A.V. Olinto, and C. Tyler, Astropart. Phys. **18**, 649 (2003).
- [23] R. Aloisio, P. Blasi, and A.V. Olinto, JCAP **0405**, 007 (2004).
- [24] D.P. Finkbeiner, astro-ph/0409027.
- [25] D. Hooper, D.P. Finkbeiner, and G. Dobler, Phys. Rev. D **76**, 083012 (2007).
- [26] D. Hooper, G. Zaharijas, D.P. Finkbeiner, and G. Dobler, Phys. Rev. D **77**, 043511 (2008).
- [27] D. Hooper, arXiv:0801.4378.
- [28] J.F. Navarro, C.S. Frenk, and S.D.M. White, Astrophys. J. **462**, 563 (1996); Astrophys. J. **490** 493 (1997).
- [29] We note that a weaker but more rigorous bound comes from unitarity of the annihilation process. The textbook unitarity bound is simply  $\sigma \leq 4\pi (2L+1)/p_{\text{cm}}^2$  for the  $l^{\text{th}}$  partial wave, from which we infer  $\langle v \sigma \rangle \leq 4\pi/(v M_\chi^2)$  for non-relativistic particles in the  $L=0$  partial wave. Substituting for the LHS from Eq. (2), one obtains  $(g_B^2/4\pi) \leq \frac{1}{\sqrt{v}} (M_B^2/M_\chi^2)$ . Thus, unitarity allows strong coupling, if it is suppressed in the amplitude by the propagator factor  $\sim M_B^{-2}$ . The bound from the perturbative assumption is not so forgiving.
- [30] For  $M_B < M_\chi$ , one finds the decay width  $\Gamma(\chi \rightarrow B + \nu) = \frac{g_B^2}{16\pi} \left(1 - \frac{M_B^2}{M_\chi^2}\right)^2 M_\chi$ .